



ELSEVIER

Thermochimica Acta 284 (1995) 179–190

thermochimica
acta

Comparison of isothermal and non-isothermal TTT-curves in the system 2,4-pentanediol in water¹

Patrick M. Mehl*

Organ Incorporated, 2434 North Greenview, Chicago, IL 60614, USA

Abstract

The system 2,4-pentanediol–water is shown to form glasses for concentrations above 30% by weight for cooling rates above $80^{\circ}\text{C min}^{-1}$. Below this concentration, ice crystallizes during the initial cooling. Ice crystallization is calorimetrically recorded in isothermal and non-isothermal conditions during either the initial cooling from the melt or the subsequent warming from the glassy state for glass-forming concentrations. Time–Temperature–Transformation (TTT) curves for a 0.1 crystallization fraction have been constructed. For 35% w/w 2,4-pentanediol in water, two “noses” are recorded for isothermal conditions. They are identified with the thermal ranges as being the consequences of homogeneous and heterogeneous ice nucleation. A comparison of isothermal and non-isothermal conditions is also presented to underline the difficulty of applying the usual “nose method” for the determination of the critical cooling and warming rates. The Johnson–Mehl–Avrami model is used for the analysis of the isothermal ice crystallization. comparison of the parameters calculated after cooling or after warming from the glassy state shows that the homogeneous nucleation occurs at a constant rate and that the heterogeneous nucleation occurs as approximately the inverse square root of the time rate.

Keywords: Crystal growth rates; Ice crystallization; Nucleation rates, 2,4-Pentanediol; TTT-curves; Water

* Corresponding address: Transfusion Research Medicine Program, Naval Medical Research Institute, Bldg. 29, Naval Medical Center, 8901 Wisconsin AV., Bethesda MD 20889-5607, USA*

¹ Presented at the 24th NATAS Conference in San Francisco, CA, USA, 10–13 September 1995

1. Introduction

The determination of critical cooling and warming rates for the formation of glassy states by suppression of crystallization in glass-forming liquids has long been a subject of discussion for various fields of applications [1–4]. The “common nose” method designed to apply isothermal conditions to non-isothermal conditions is well known [1–4]. This method has been applied for glass-forming aqueous solutions with apparent good accord with previous investigations for aqueous solutions using emulsion systems [5, 6]. Emulsion systems were also used for the determination of the ice nucleation kinetics [5, 6]. This method is tested here for the system 2,4-pentanediol–water.

2,4-Pentanediol was reported to be a good glass-former [7–9]. As a solute in water, the crystallization of its eutectic is therefore expected to be strongly suppressed. A partial solid–liquid phase diagram has been previously reported with the determination of the homogeneous ice nucleation and of the ice crystal growth rates [10]. The glass-forming concentration range for this system has been previously found [10] and was checked in the present study before the determination of the TTT-curves. TTT-curves have been used for the determination of critical cooling rates and critical warming rates for glass-forming solutions [5, 6]. A previous study has reported the kinetics of ice nucleation for dilute solutions of 2,4-pentanediol in water using an emulsion system. The emulsified solution samples had the advantage of providing a direct measure of the ice nucleation kinetics [10]. However, the possibility of forming a stable emulsion decreases with increasing solute concentration. Therefore bulk solution samples were tested as they provide a more general crystallization, with the possible growth of heterogeneous or homogeneous ice nuclei. For these bulk samples, the Johnson–Mehl–Avrami model can be applied to the isothermal crystallization in samples with various thermal histories.

2. Materials and methods

2.1. Sample preparation

2,4-Pentanediol (99%, mixture of isomers, Aldrich) and deionized water were used without further purification for the preparation of the samples. Bulk samples of 30, 35, 40 and 45% w/w concentration were prepared. The samples weighed between 10 and 20 mg. They were placed in a Perkin-Elmer DSC-4 for the determination of ice crystallization peaks. This calorimeter was calibrated as usual [11], using first-order and melting transitions of pure organic compounds.

2.2. Analysis using the JMA model

Analysis of the bulk sample data was carried out using the Johnson–Mehl–Avrami (JMA) model which was shown to fit the data under isothermal experimental conditions. Uhlmann reported the general equation governing the JMA model, combining

the nucleation rate $J(T)$ and the crystal growth rate $U(T)$ [12] to express the crystallization fraction $X(T, t)$ at the temperature T after an annealing time t , where $X(T, t)$ was defined as the ratio (heat of crystallization at time t)/(total heat of crystallization) to approximate the volume ratio of ice crystallization

$$X(T, t) = 1 - \exp \left[- \int_0^t J(T, t') \alpha(m) \left[\int_{t'}^t U(T, t'' - t') dt'' \right]^m dt' \right] \quad (1)$$

where α is a function dependent on the dimensionality m of the ice crystals. Eq. (1) can be reduced to a simpler equation [12]

$$X(T, t) = - \exp [- (K(T)t)^n] \quad (2)$$

with n as the Avrami exponent, n being a function of the scaling of the nucleation rate with time and of the dimension m , and the constant of crystallization $K(T)$ is

$$K(T) = K_o (T_m - T) \exp \left[- \frac{E_a}{R\Theta} \right] \quad (3)$$

with Θ equal to T or to $T - T_k$ for an Arrhenius or a Vogel–Fulcher–Tamman representation. Analysis of the Avrami exponent can result in interesting conclusions concerning the kinetics of the ice nucleation.

The dimension m is assumed to be dependent on the temperature T alone and not on the time of growth, which is a similar condition for self-similarity growth for fractal growth observed in snow flakes. The isothermal experiments were performed after the initial cooling from the melt or after subsequent warming from the glassy state. During warming from the glassy state, it is observed by cryomicroscopy that ice crystals have all the same size and shape. Therefore, during annealing for isothermal conditions from the glassy state, $J(T) = 0$. Therefore, its associated integral in the JMA model is a constant equal to the number of ice nuclei per unit of volume. For isothermal conditions from the melt, $J(T)$ is no longer equal to 0. Then the Avrami exponent will reflect a variation due to the variation of the ice nucleus density. Ice nucleation rates can be theoretically deduced from the ratio of the crystallization constants from the JMA parameters. For glassified samples prior to isothermal crystallization, it was assumed that ice nuclei formed during the initial cooling at temperatures suppressing the ice crystal growth.

Assuming that the ice crystal growth rates are represented by the following relation previously reported by Doremus [13], for pure melts and for aqueous solutions [14, 15]

$$U(T) = A(T_m - T) \exp \left(- \frac{E_{ag}}{RT} \right) \quad (4)$$

The classical ice nucleation kinetics [16] can also be approximately represented by

$$J(T) = \left[B \exp \left[- \frac{C}{F(T)} \right] \exp \left[- \frac{E_{ag}}{RT} \right] (t - t_{ind}) \right]^\beta \quad (5)$$

where $J(T)$ is the nucleation rate per unit of volume at the temperature T , C is a constant depending on the heat of fusion and the solid–liquid surface free energy, and

$F(T)$ is a function of the melting temperature and T . The second exponential function is introduced for the viscosity of the solution, as for ice crystal growth rates. Eq. (5) can be simplified for the calculation to a simple Arrhenius form with an apparent activation energy E_{an} for temperatures sufficiently low to favor the viscosity term in the expression. The combination of Eqs. (4) and (5) in Eq. (3) for isothermal conditions provides the system

$$mE_{ag} + \beta E_{an} \quad \text{with} \quad m + \beta + 1 = n \quad (6)$$

For the isothermal ice crystallization from the glassy state in glass-forming aqueous solutions, cryomicroscopic observations show that the size of all ice crystals are identical at the reading error. This indicates that the nucleation rate is null for isothermal conditions from the glassy state; $\beta = 0$ for these conditions and $J(T) = 0$, providing the direct measure of $m = n$ and $E_{ag} = E_a$. For the isothermal conditions from the melt, the nucleation rate is not considered as equal to 0 and leads to the determination of the other parameters. It is, however, assumed that the characteristics of the ice crystal growth are identical in both isothermal conditions, from the melt and from the glassy state.

The calculated parameters describing the non-isothermal crystallization are expected to have different values from those for isothermal conditions. The introduction of the time dependence of the temperature will significantly change the integration with the introduction of the exponential integral function due to the presence of both exponential functions of $1/RT$. The dependence of the fraction X on temperature has not been introduced. X is dependent on the solute concentration and that of the solution after total crystallization at temperature T . The resolution of the integral equation is not presented here [17].

2.3. Determination of the TTT-curves

The ice crystallization peaks were recorded calorimetrically and the crystallization heat measured as a function of the annealing time. As a function of the annealing time, the various parameters (n , E_a , K_0) for the JMA model can be determined for each isothermal annealing experiment, either after cooling from the melt or after warming from the glassy state. To remain within the sensitivity of the DSC-4, a 0.1 ratio was chosen for the determination of the TTT-curves. Trying to determine experimentally a smaller fraction increases the reading errors, which might exceed the sensitivity of the calorimeter. These TTT-curves are defined as the corresponding annealing time at the annealing temperature at which the crystallization fraction is 10%. It is assumed that the heat of crystallization fraction and the crystallization fraction are identical.

Similar non-isothermal TTT-curves can be defined as the curves with a corresponding temperature T at which, during cooling, the crystallization fraction is observed to be 0.1. The time is then replaced by the time spent by the sample below the melting temperature during cooling at various rates and, eventually, during warming at various rates, assuming an exposure time equal to zero below the glass transition to reach the corresponding temperature T . The same ratio of 0.1 is chosen for the comparison between isothermal and non-isothermal conditions. These similar TTT-curves have

been previously used by MacFarlane for developing his model of diffusion-controlled ice crystallization for continuous cooling using the additive concept [18]. However, the determination of the critical cooling rates is more complex than the determination using the technique of the nose time [19].

3. Results and discussion

3.1. Phase diagram and ice crystallization

The various phase transitions were recorded by calorimetry and are reported in Fig. 1. Only ice was observed to crystallize at the sensitivity of the calorimeter. The heat of crystallization during the initial cooling is reported in Fig. 2 as a function of the cooling rate for various concentrations of 2,4-pentanediol in water.

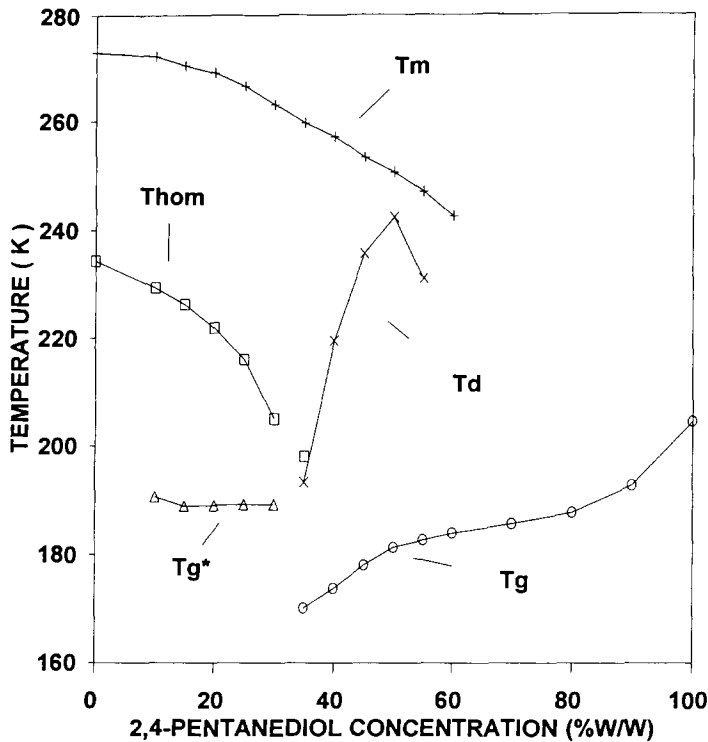


Fig. 1. Phase diagram of the 2,4-pentanediol–water system measured by calorimetry during warming at $10^{\circ}\text{C min}^{-1}$: \circ , glass transition T_g of the vitrified solution without crystallized ice; Δ , glass transition T_g^* of the partially vitrified solution after total crystallization; x , devitrification temperature T_d at maximum rate of crystallization during warming; $+$, melting temperature T_m . T_{hom} (\square) was measured during cooling at $2.5^{\circ}\text{C min}^{-1}$.

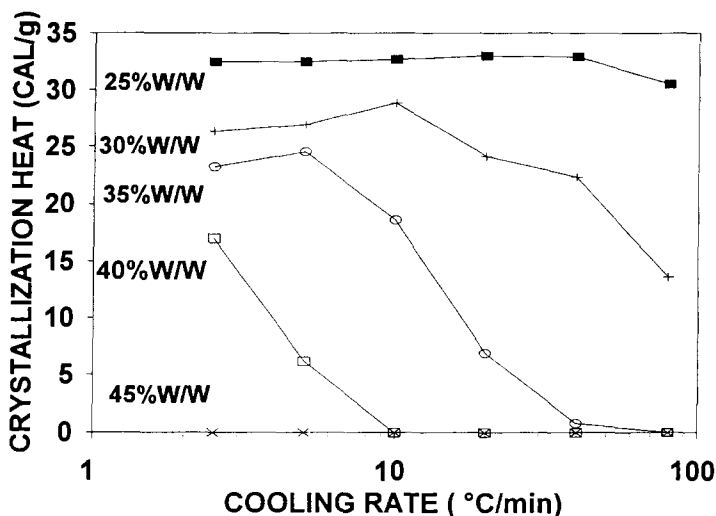


Fig. 2. Heat of crystallization (J/g of solution) recorded during cooling as a function of the cooling rate for various concentrations of 2,4-pentenediol in water.

3.2. TTT-curves

TTT-curves for the isothermal conditions during the initial cooling are reported in Fig. 3 for various solute concentrations. As reported in a theoretical model by Weinberg [20], observations of more than one “nose” for the TTT-curves are the possible consequence of a combined homogeneous and heterogeneous nucleation. The

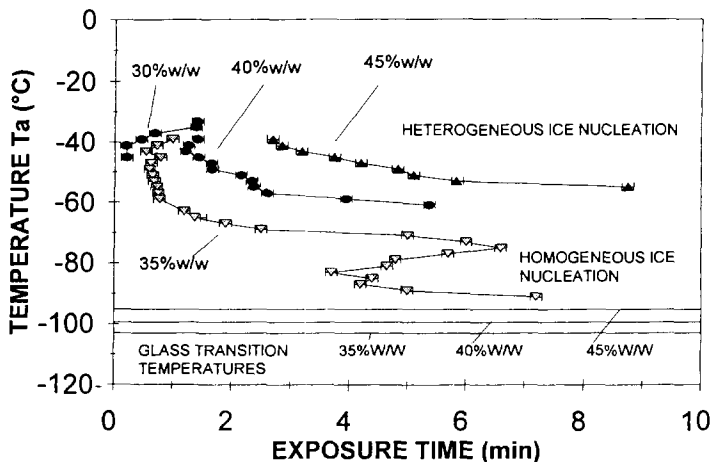


Fig. 3. Isothermal TTT-curves for a crystallization fraction of 0.1 for various concentrations of 2,4-pentenediol in water. The samples were cooled directly from the melt to the annealing temperature.

higher annealing temperatures are also limited by an induction time of the various heterogeneous ice nuclei. The induction time is longer as supercooling is decreased [21]. This induction time is observed here, with delayed crystallization, resulting in multiple peaks associated with various ice nuclei. Below this first “nose” at the higher temperature, the time of the TTT-curve increases due to the increase in the solution viscosity which lowers the ice crystal growth. The only possibilities for a decrease in the time for these TTT-curves, at these low temperatures, are either an increase in the ice crystal growth, which is excluded for one single liquid phase as seen before, due to the solution viscosity, or an increase in the ice nucleus density, as for the homogeneous ice nucleation. The onset temperature of the second “nose” is $-75^{\circ}\text{C} \pm 2^{\circ}\text{C}$. This temperature is a few degrees higher than the extrapolated value of the calorimetric onset homogeneous nucleation temperature obtained from the previously reported phase diagram [22]. Therefore, the second “nose” at the lowest temperatures corresponds to the homogeneous nucleation.

The TTT-curves for isothermal conditions during warming are reported in Figs. 4–6 for 35, 40 and 45% w/w solute, with a comparison with those from Fig. 3. The annealing time to achieve the same crystallization ratio is shorter for the isothermal conditions during warming from the glassy state. This indicates higher ice nucleus densities within the samples in the glassy state. To reach the glassy state, the solution has crossed the whole homogeneous ice nucleation thermal range. Because the ice crystal growth thermal range is higher than for the homogeneous ice nucleation, the ice nuclei will not grow and the number of ice nuclei will not change during the present time of annealing (5–10 min exposure) from the glassy state.

The comparison of the TTT-curves on cooling from the melt and on warming from the glassy state with those during continuous cooling conditions are reported in Figs. 7

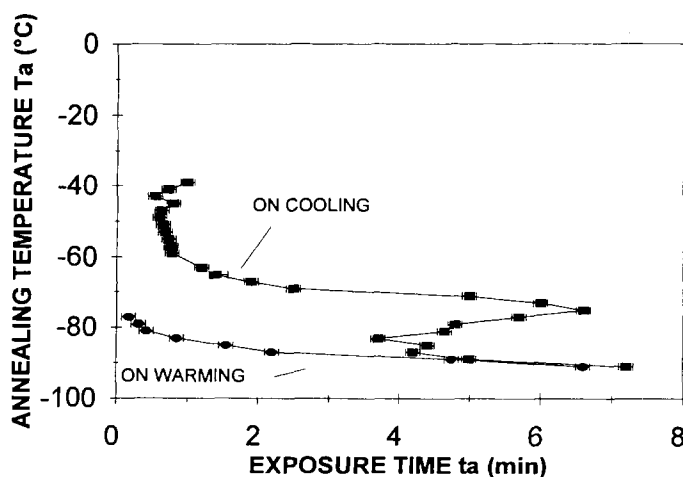


Fig. 4. Comparison of the isothermal TTT-curves for a crystallization fraction of 0.1 for 35% w/w 2,4-pentanediol in water on cooling from the melt (■) and on warming from the glassy state (●). The samples were cooled at $80^{\circ}\text{C min}^{-1}$ which is sufficient to achieve vitrification of the solution [12].

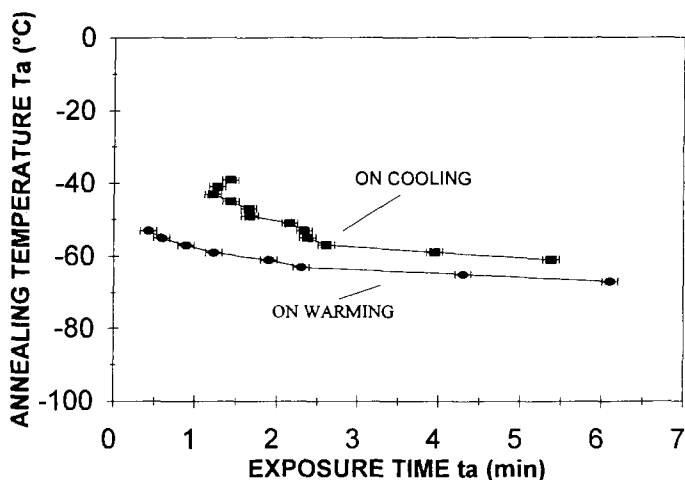


Fig. 5. Comparison of the isothermal TTT-curves for a crystallization fraction of 0.1 for 40% w/w 2,4-pentandiol in water on cooling from the melt (■) and on warming from the glassy state (●). The samples were cooled at $40^{\circ}\text{C min}^{-1}$ which is sufficient to achieve vitrification of the solution [12].

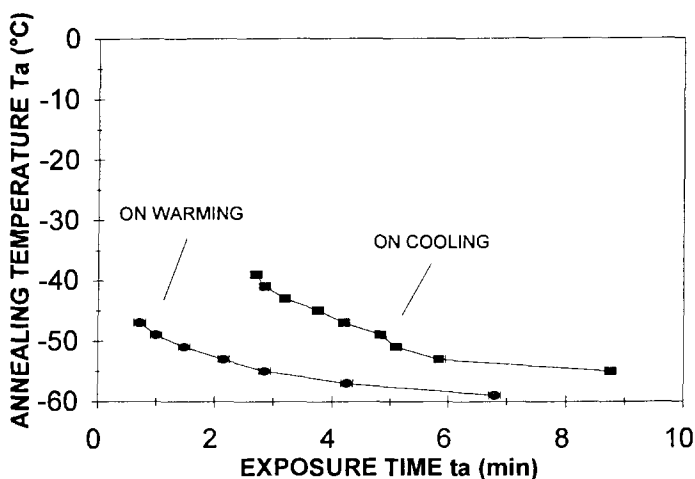


Fig. 6. Comparison of the isothermal TTT-curves for a crystallization fraction of 0.1 for 45% w/w 2,4-pentandiol in water on cooling from the melt (■) and on warming from the glassy state (●). The samples are cooled at $20^{\circ}\text{C min}^{-1}$ which is sufficient to achieve vitrification of the solution [12].

and 8 for, respectively, 35 and 40% w/w 2,4-pentandiol in water. For 45% w/w 2,4-pentandiol in water, the TTT-curves are similar to those reported in Fig. 8 for 40% w/w solute. Differences between isothermal and non-isothermal conditions are expected to exist because the integration with time within Eq. (1) is different, as the temperature of the sample is also time dependent. The straight lines represent the rates

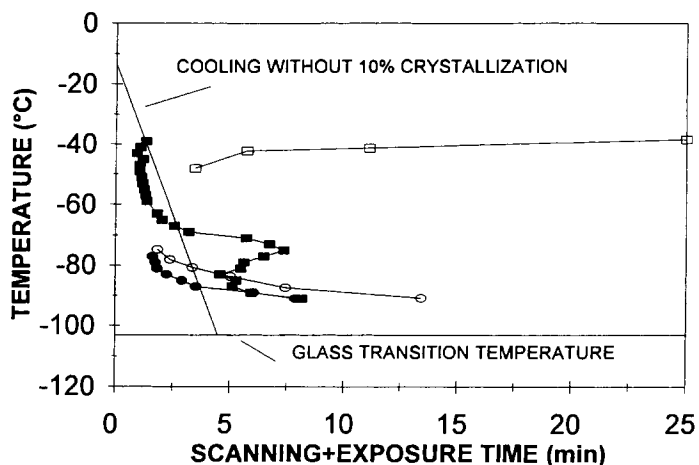


Fig. 7. Comparison of the combined isothermal (Fig. 4) and continuous cooling (CT) TTT-curves for a crystallization fraction of 0.1 for 35% w/w 2,4-pentandiol in water on cooling from the melt (■) and on warming from the glassy state (●). For CT conditions on cooling, (□), the samples were cooled at various rates down to the glass transition. For CT conditions on warming (○), the samples were cooled at $80^{\circ}\text{C min}^{-1}$ which is sufficient to achieve vitrification of the solution [12] before warming them at various warming rates.

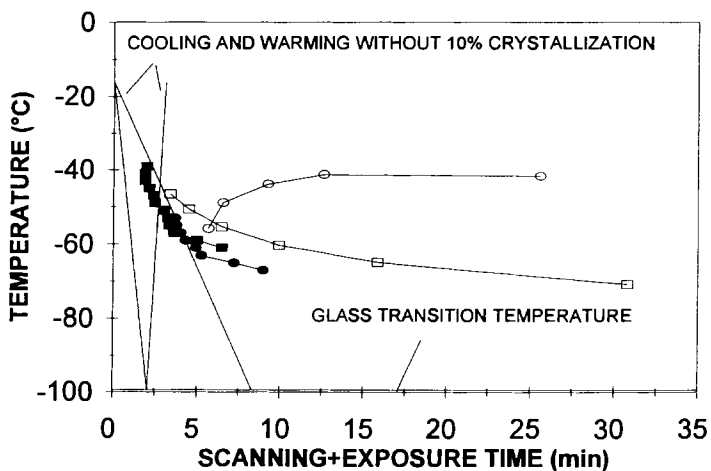


Fig. 8. Comparison of the combined isothermal (Fig. 5) and continuous cooling (CT) TTT-curves for a crystallization fraction of 0.1 for 40% w/w 2,4-pentandiol in water on cooling from the melts (■) and on warming from the glassy state (●). For CT conditions on cooling (○), the samples were cooled at various rates down to the glass transition. For CT conditions on warming (□), the samples were cooled at $40^{\circ}\text{C min}^{-1}$ which is sufficient to achieve vitrification of the solution [12] before warming them at various warming rates.

needed to suppress the crystallization of ice to 10%. These straight lines cross the isothermal TTT-curves. The ice crystallization is, therefore, slower for constant cooling or warming than during isothermal exposure.

3.3. Analysis of the kinetics

The analysis of the ice crystallization using the JMA model provides a set of parameters for each of the experimental conditions which are reported in Table 1. The values of these parameters are determined either during cooling or during warming, and compared to determine the various values of m , α , E_{ag} , and E_{an} . The errors of determination for the exponents and for the activation energies are very high in comparison with those for the direct measurements. The direct determination of the ice crystal growth rates by cryomicroscopy provides general activation energies, E_a using Eq. (4), and are also reported in Table 1. These activation energies increase slightly with the solute concentration and are directly related to the inverse of the viscosity of the solution. However, there is a curvature to the crystal growth rates due to the better Vogel–Fulcher–Tamman representation of the viscosity of solution.

The local activation energies for crystal growth, in the same thermal ranges as used in calorimetry will also decrease with the solute concentration. The curvature will provide a lower tangent slope as the temperature increases. The constancy of the crystal growth indicates an interface-controlled kinetics [23] which is different from the diffusion-controlled theory presented by MacFarlane [18]. This constancy is observed here for

Table 1
Parameters of the JMA model for ice crystallization in various concentrations C (% w/w) of 2,4-pentanediol in water

$c/\%$ w/w	35	40	45
On cooling			
n	3.21 ± 0.32	3.09 ± 0.10	3.36 ± 0.19
$E_a/(\text{kJ mol}^{-1})$	36.5 ± 1.7	43.9 ± 1.6	46.1 ± 2.6
K_0/s^{-1}	$2.7 \pm 0.2 \text{ E5}$	$1.9 \pm 0.1 \text{ E6}$	$2.4 \pm 0.2 \text{ E6}$
On warming			
n	2.35 ± 0.26	2.44 ± 0.18	2.74 ± 0.15
$E_a/(\text{kJ mol}^{-1})$	77.2 ± 1.8	72.1 ± 0.8	74.1 ± 0.6
K_0/s^{-1}	$3.3 \pm 0.6 \text{ E17}$	$6.5 \pm 0.1 \text{ E13}$	$8.6 \pm 0.1 \text{ E13}$
Calculated values			
$n(\text{cool.})-n(\text{warm.})$	0.86 ± 0.45	0.65 ± 0.12	0.61 ± 0.25
m	2.35 ± 0.25	2.44 ± 0.18	2.74 ± 0.15
β	-0.14 ± 0.45	-0.35 ± 0.12	-0.39 ± 0.25
$E_{ag}/\text{kJ mol}^{-1}$	77.2 ± 1.8	72.1 ± 0.8	74.1 ± 0.6
$E_{an}^a/\text{kJ mol}^{-1}$	461.1 ± 293.3	115.0 ± 69.3	122.4 ± 77.6
From cryomicroscopic analysis of crystal growth [15]			
$E_{ag}/\text{kJ mol}^{-1}$	70.0 ± 0.8	70.0 ± 1.7	81.2 ± 5.0

^a Calculated from the mean value of β .

high supercooling and for high solute concentrations. For low solute concentrations and for low supercoolings, the growth rates are dependent on the size of the ice crystals, indicating diffusion-controlled kinetics of the growth. These different observations lead to difficulties in the interpretation of the thermal data recorded by calorimetry.

The difference in the Avrami exponent from cooling and from warming is close to 1 for 35% w/w and close to 0.5 for higher concentrations. The fact that ice nuclei may already be present during the initial cooling will lower this difference to lower values for 35% w/w solute. The nucleation rate is constant for homogeneous ice nucleation and is proportional to $(t - t_{\text{ind}})^{-0.50}$ for heterogeneous ice nucleation. One must note, however, that the thermal range used for the comparison of the various parameters has been chosen below the “nose” of the TTT-curves, which may limit the interpretation of the isothermal data from cooling. Indeed, the ice nucleation will be lower below the TTT-curve and be subject to the viscosity approximation made in the Method section for the ice nucleation.

4. Conclusion

Isothermal TTT-curves for bulk samples are very informative for localization of the heterogeneous and homogeneous ice nucleation for aqueous glass-forming solutions. Isothermal TTT-curves have been previously determined using emulsion techniques for the separation of both nucleation processes [5, 6]. However this technique is limited to relatively low solute concentrations so as to produce stable emulsions and also to solutes that are slightly hydrophobic.

A comparison of the kinetics parameters during isothermal crystallization between samples cooled from the melt and those warmed from the glassy state shows that the kinetics of ice nucleation can be partially determined. Eq. (7) shows that for glass-forming solutions, isothermal crystallization after warming from the glassy state is primarily the consequence of crystal growth compared to the isothermal crystallization after cooling from the melt. This is a superimposition of the ice nucleation and of the ice crystal growth. These glass-forming aqueous solutions usually have their homogeneous nucleation below the thermal range of the crystal growth. This is observed by comparing the activation energies with the direct measurement by cryomicroscopy of the crystal growth [15]. These activation energies are relatively similar for cryomicroscopic measurements of the crystal growth rates and the isothermal crystallization from the glassy state by calorimetry. A slight difference exists with 35% w/w 2,4-pentanediol in water. This may be due to a slight overlap of the homogeneous ice nucleation and ice crystal growth thermal ranges.

The “nose method”, using isothermal TTT-curves to determine critical cooling and warming rates, will provide higher rate values than those for the real effective critical rates. The fundamental differences between the isothermal and non-isothermal conditions are apparent by considering the relationship between temperature and time. This observation has recently been discussed and shows that the determination of the critical rates is more likely to be dependent on the viscosity of the solution [19]. Moreover, the existence of an induction time either for nucleation or for growth, which

is temperature dependent during the initial cooling, introduces a delay term in the heterogeneous nucleation during continuous cooling [24, 25]. During warming from the glassy state, the ice nucleation is very slow before reaching the thermal ranges of relatively high crystal growth rate.

Acknowledgements

The author would like to thank Dr. H.T. Meryman for his continuous support. This research has been conducted under the terms of the Cooperative Research And Development Agreement signed the 01/15/95 between the Naval Medical Research Institute and Organ Incorporated, with the Naval Medical Research and Development Command Work Unit No N6422394RC64.

The opinions and assertions contained herein are those of the author and are not to be construed as official nor as representing those of the Department of Defense nor of the Navy.

References

- [1] M.C. Weinberg, D.R. Uhlmann and E.D. Zanotto, *J. Am. Ceram. Soc.*, 72 (1989) 2054.
- [2] C.A. Angell and Y. Choi, *J. Microsc.*, 141 (1986) 251.
- [3] D.R. MacFarlane and C.A. Angell, *J. Phys. Chem.*, 86 (1982) 1927.
- [4] D.R. MacFarlane, C.A. Angell and R.K. Kadiyala, *J. Chem. Phys.*, 79 (1983) 3921.
- [5] M. Kresin and C. Körber, *J. Chem. Phys.*, 95 (1991) 5249.
- [6] R.L. Sutton, *Cryo-Lett.*, 11 (1990) 49.
- [7] G. Fytas and T. Dorfmüller, *Ber. Bunsenges. Phys. Chem.*, 85 (1981) 1064.
- [8] G. Fytas and T. Dorfmüller, *J. Chem. Phys.*, 75 (1981) 5232.
- [9] G. Fytas and T. Dorfmüller, *Mol. Phys.*, 47 (1982) 741.
- [10] P.M. Mehl, *Cryobiology*, in press.
- [11] P.M. Mehl, *Cryobiology*, 30 (1993) 509.
- [12] D.R. Uhlmann, in A.F. Wright and J. Dupuy (Eds), *Glass ... Current Issues*, NATO ASI Serie E # 92, Martinus Nijhoff Pub., Dordrecht, 1985, p. 1.
- [13] R.H. Doremus, *Glass Science*, Wiley, London, 1973.
- [14] P. Boutron and A. Kaufmann, *Cryobiology*, 16 (1979) 83.
- [15] P.M. Mehl, *J. Cryst. Growth*, in press.
- [16] F. Franks, in F. Franks (Ed.), *Water, A Comprehensive Treatise*, Vol. 7, Plenum Press, New York, 1982, Chap. 3, p. 215.
- [17] P.M. Mehl, *Thermochim. Acta*, 223 (1993) 157.
- [18] D.R. MacFarlane, *J. Non-Cryst. Solids*, 53 (1982) 61.
- [19] M.C. Weinberg, *J. Non-Cryst. Solids*, 167 (1994) 81.
- [20] M.C. Weinberg, *J. Am. Ceram. Soc.*, 75 (1992) 56.
- [21] V.A. Shneidman and M.C. Weinberg, *J. Chem. Phys.*, 97 (1992) 3621.
- [22] S. Charoenrein and D.S. Reid, *Thermochim. Acta*, 156 (1989) 373.
- [23] J. Hey, Ph.D. Thesis, Monash University, Victoria, Australia, 1995.
- [24] J. Deubener, R. Bruckner and M. Sternitzke, *J. Non-Cryst. Solids*, 163 (1993) 1.
- [25] M.C. Weinberg, *J. Non-Cryst. Solids*, 170 (1994) 300.